文章编号:1000-0887(2014)05-0510-13　

耦合载荷冲击下圆柱壳的动态屈曲*

马建青[1], 徐新生[2]

(1. 西安石油大学 机械工程学院, 西安 710065;
2. 大连理工大学 工程力学系;工业装备结构分析国家重点实验室, 辽宁 大连 116024)

摘要: 考虑轴向、扭转耦合应力波在圆柱壳中的传播,对弹性长圆柱壳动态屈曲问题进行了探讨.首先建立问题的 Hamilton(哈密顿)体系,在此基础上,临界屈曲载荷和屈曲模态转化为辛空间中的辛本征值和本征解问题,借助于 Hamilton 体系的性质和完备性给出了一个完备的屈曲模态空间,揭示了各临界载荷和屈曲模态在辛体系中与辛本征值和本征解的对应关系.长圆柱壳在轴向和扭转耦合冲击载荷下的动态屈曲,由于轴向应力波和扭转应力波传播速度不同,使得应力纵波和横波在圆柱壳的传播与反射中不同步,圆柱壳被分成多个区域,每个区域的应力、位移和边界条件各不相同.数值结果给出了固支及简支边界条件下圆柱壳的临界载荷曲线和屈曲模态,着重探讨了不同类型的一阶屈曲模态.

关　键　词: Hamilton 体系; 圆柱壳; 动态屈曲; 耦合冲击; 应力波
中图分类号: O343.9　　**文献标志码**: A
doi: 10.3879/j.issn.1000-0887.2014.05.005

引　　言

薄壁结构的屈曲问题一直是结构工程师和结构力学家们所关注的课题,圆柱壳作为工程中常用的基本构件,在耦合冲击载荷作用下的动态屈曲问题也是工程中的重要问题,一直受到人们的关注.Bisagni 等[1-2]通过实验分析了薄壁碳纤维复合材料圆柱壳的前屈曲及后屈曲问题,对圆柱壳分别加载轴向载荷、扭转载荷以及两种载荷耦合情形,并且也对轴压和扭转载荷共同作用下加筋圆柱壳的后屈曲进行了理论分析和实验研究,给出了具有工程参考价值的实验数据.Miyazaki[3]用有限元方法分析了轴压与内外压的临界时间及屈曲模式.Azam[4]考虑脱层接触影响,应用有限元方法分析了轴压脱层圆柱壳的屈曲以及外压圆柱壳的前屈曲和后屈曲问题.Diaconu 等[5]采用 Flügge 理论研究了在轴向和扭转载荷共同作用下层合圆柱壳的屈曲行为.黄承义等[6]根据实验结果,采用 Lagrange 方法分析了有限长薄圆柱壳在余弦冲击载荷作用下的弹性脉冲动力屈曲.吴斌等[7]在正交异性圆柱壳的轴对称运动方程中考虑剪切变形和转动惯性,应用广义特征线理论得到沿特征线上的相容方程,采用数值积分计算了受轴向冲击和扭转联合作用下有限长圆柱壳的波传问题.王德禹等[8]推导了圆柱壳塑性动力扭转屈曲线性方程,获得了临界冲击速度.

1　基 本 问 题

考虑承受轴向和扭转冲击载荷作用的圆柱壳(如图 1),半径为 R,厚度为 h,长度为 l,密度

---

* **收稿日期**: 2013-08-08; **修订日期**: 2013-12-10
作者简介: 马建青(1977—),女, 河北望都人, 博士(通讯作者. E-mail: majianqing2000@163.com).

为 ρ,弹性模量为 E,Poisson(泊松) 比为 μ,选取柱坐标系 (x,θ,r),对应的位移为 (u,v,w).

内力和弯矩与曲率关系以及几何关系可以写成:

$$\begin{cases} N_x = K(\varepsilon_x + \mu\varepsilon_\theta), \\ N_\theta = K(\varepsilon_\theta + \mu\varepsilon_x), \\ N_{x\theta} = K(1-\mu)\varepsilon_{x\theta}/2, \\ M_x = D(\kappa_x + \mu\kappa_\theta), \\ M_\theta = D(\kappa_\theta + \mu\kappa_x), \\ M_{x\theta} = D(1-\mu)\kappa_{x\theta}; \end{cases} \qquad \begin{cases} \varepsilon_x = \partial_x u, \\ \varepsilon_\theta = \partial_\theta v + w/r, \\ \varepsilon_{x\theta} = \partial_\theta u + \partial_x v, \\ \kappa_x = -\partial_x^2 w, \\ \kappa_\theta = -\partial_\theta^2 w + \partial_\theta v/r^2, \\ \kappa_{x\theta} = -\partial_x\partial_\theta w + \partial_x v/(2r), \end{cases} \tag{1}$$

其中抗拉刚度 $K = Eh/(1-\mu^2)$,抗弯刚度 $D = Eh^3/(12(1-\mu^2))$,$\partial_x \equiv \partial/\partial x$,$\partial_\theta \equiv \partial/(r\partial\theta)$.

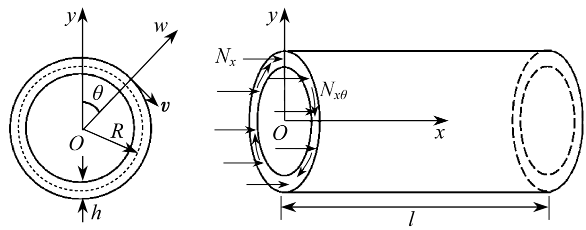

图 1　受耦合冲击的圆柱壳

Fig.1　Geometrical parameters of a cylindrical shell under coupled impact

圆柱壳体的应变势能密度为

$$U = \frac{K}{2}\left(\varepsilon_x^2 + \varepsilon_\theta^2 + 2\mu\varepsilon_x\varepsilon_\theta + \frac{1-\mu}{2}\varepsilon_{x\theta}^2\right) + \frac{D}{2}(\kappa_x^2 + \kappa_\theta^2 + 2\mu\kappa_x\kappa_\theta + 2(1-\mu)\kappa_{x\theta}^2) + \frac{N_x}{2}\left(\frac{\partial w}{\partial x}\right)^2 + \frac{N_{x\theta}}{R}\frac{\partial w}{\partial x}\frac{\partial w}{\partial \theta}. \tag{2}$$

动能密度为

$$V = \frac{1}{2}\rho h\left(\frac{\partial u}{\partial t}\right)^2 + \frac{1}{2}\rho h\left(\frac{\partial v}{\partial t}\right)^2 + \frac{1}{2}\rho h\left(\frac{\partial w}{\partial t}\right)^2. \tag{3}$$

考虑薄壳发生前屈曲时,端部承受均匀轴向和扭转载荷,由壳体内能、外力功、动能组成的 Lagrange 函数为

$$\begin{aligned}\tilde{L} = \iint\Big\{ &\frac{1}{2}\rho h\left(\frac{\partial u}{\partial t}\right)^2 + \frac{1}{2}\rho h\left(\frac{\partial v}{\partial t}\right)^2 + \frac{1}{2}\rho h\left(\frac{\partial w}{\partial t}\right)^2 - \\ &\frac{K}{2}\left(\varepsilon_x^2 + \varepsilon_\theta^2 + 2\mu\varepsilon_x\varepsilon_\theta + \frac{1-\mu}{2}\varepsilon_{x\theta}^2\right) - \\ &\frac{D}{2}(\kappa_x^2 + \kappa_\theta^2 + 2\mu\kappa_x\kappa_\theta + 2(1-\mu)\kappa_{x\theta}^2) - \frac{N_x}{2}\left(\frac{\partial w}{\partial x}\right)^2 - \frac{N_{x\theta}}{R}\frac{\partial w}{\partial x}\frac{\partial w}{\partial \theta}\Big\} R\mathrm{d}\theta\mathrm{d}x. \end{aligned} \tag{4}$$

Hamilton 作用量 $J = \int \tilde{L}\mathrm{d}t$, 由 Hamilton 变分原理 $\delta\int\tilde{L}\mathrm{d}t = 0$ 得到.

上式对 u 变分,可以得到波动方程:

$$\frac{\partial^2 u}{\partial t^2} - c_1^2\frac{\partial^2 u}{\partial x^2} = 0,$$

其中 $c_1 = [E/(\rho(1-\mu^2))]^{1/2}$, 为应力波纵波波速.

对 v 变分,不考虑 u,w 方向位移,可以得到波动方程:

$$\frac{\partial^2 v}{\partial t^2} - c_2^2 \frac{\partial^2 v}{\partial x^2} = 0,$$

其中 $c_2^2 \approx E/[2\rho(1+\mu)]$，$c_2$ 为扭转应力波波速。

考虑壳体在冲击端 ($x = 0$) 作用有轴向和扭转藕合冲击载荷：

$$\begin{cases} N_x(0,t) = -N\mathrm{H}(t), \\ N_{x\theta}(0,t) = T\mathrm{H}(t), \end{cases}$$

其中 N, T 是常数，$\mathrm{H}(t)$ 是时间的阶梯函数：

$$\mathrm{H}(t) = \begin{cases} 1, & t \geqslant 0, \\ 0, & t < 0. \end{cases}$$

轴向冲击载荷以波速 $c_1 = [E/(\rho(1-\mu^2))]^{1/2}$ 在圆柱壳内传播，扭转冲击载荷以波速 $c_2 = [E/(2(1+\mu)\rho)]^{1/2}$ 在圆柱壳内传播，波速 $c_2 < c_1$。圆柱壳的内力由轴力和剪力组合而成。如果不考虑应力波的反射，圆柱壳应分为 3 个区域：

$$\begin{cases} 0 \leqslant x \leqslant c_2 t, & \text{应力纵波和横波耦合作用区}, \\ c_2 t \leqslant x \leqslant c_1 t, & \text{应力纵波作用区}, \\ c_1 t \leqslant x \leqslant l, & \text{非扰动区}. \end{cases}$$

在这 3 个区域，应力分别为

耦合作用区

$$\begin{cases} N_x = -N, \\ N_{x\theta} = T, \end{cases} \quad 0 \leqslant x \leqslant c_2 t;$$

纵波作用区

$$\begin{cases} N_x = -N, \\ N_{x\theta} = 0, \end{cases} \quad c_2 t \leqslant x \leqslant c_1 t;$$

非扰动区

$$\begin{cases} N_x = 0, \\ N_{x\theta} = 0, \end{cases} \quad c_1 t \leqslant x \leqslant l.$$

2 Hamilton 体系

令

$$X = x/R,\ W = w/R,\ U = u/R,\ V = v/R,\ \gamma = 12\,(R/h)^2,\ L = l/r,$$
$$T = c_1 t/R,\ N_{\mathrm{cr}}(t) = N_x(t)R^2/D,\ T_{\mathrm{cr}}(t) = N_{x\theta}(t)R^2/D,$$

进行无量纲化。将 θ 坐标模拟时间坐标，即

$$\dot{(\ )} = \frac{\partial}{\partial\theta}(\ ) \equiv \partial_\theta(\ ),\ \frac{\partial}{\partial X}(\ ) \equiv \partial_X(\ ).$$

考虑在某一时刻圆柱壳的前屈曲问题，因此可忽略惯性项。引入 $\varphi = -\dot{W} + V$，则 Lagrange 函数可写为

$$\tilde{L}(U,V,W) = \frac{\gamma}{2}\left\{(\partial_X U + \dot{V} + W)^2 - 2(1-\mu)\left[\partial_X U(\dot{V} + W) - \frac{1}{4}(\dot{U} + \partial_X V)^2\right]\right\} +$$
$$\frac{1}{2}\left\{(\partial_X^2 W - \dot{\varphi})^2 - 2(1-\mu)\left[\ddot{W}\partial_X^2 W - (\partial_X \dot{W})^2 - \dot{V}\partial_X^2 W + \partial_X V \partial_X \dot{W} - \right.\right.$$

$$\left.\left.\frac{1}{4}(\partial_X V)^2\right]\right\} + (\partial_X^2 \dot{W} - \ddot{\varphi})(-\dot{W} + V - \varphi) + T_{cr}\dot{W}\partial_X W + \frac{N_{cr}}{2}(\partial_X W)^2. \tag{5}$$

定义　原变量

$$\boldsymbol{q} = \{U, V, W, \varphi\}^{\mathrm{T}} \equiv \{q_1, q_2, q_3, q_4\}^{\mathrm{T}},$$

对偶变量

$$\boldsymbol{p} = \{p_1, p_2, p_3, p_4\}^{\mathrm{T}} \equiv \{N_{x\theta}, N_\theta, Q, M\}^{\mathrm{T}}$$

分别为

$$\begin{cases} p_1 = \dfrac{\delta \tilde{L}}{\delta \dot{U}} = \dfrac{\gamma(1-\mu)}{2}(\dot{U} + \partial_X V),\ p_2 = \dfrac{\delta \tilde{L}}{\delta \dot{V}} = \gamma(\dot{V} + W + \mu\partial_X U), \\ p_3 = \dfrac{\delta \tilde{L}}{\delta \dot{W}} = -(\partial_X^2 \dot{W} - \ddot{\varphi}) + T_{cr}\partial_X W,\ p_4 = \dfrac{\delta \tilde{L}}{\delta \dot{\varphi}} = \dot{\varphi} - \partial_X^2 W. \end{cases} \tag{6}$$

方程(6)可以改写为

$$\dot{q}_1 = \frac{2p_1}{\gamma(1-\mu)} - \partial_X q_2,\ \dot{q}_2 = \frac{p_2}{\gamma} - q_3 - \mu\partial_X q_1,\ \dot{q}_3 = -q_4 + q_2,\ \dot{q}_4 = p_4 + \partial_X^2 q_3. \tag{7}$$

用原变量和对偶变量表示的 Hamilton 函数为

$$\begin{aligned} H(\boldsymbol{q},\boldsymbol{p}) &= \boldsymbol{p}^{\mathrm{T}}\dot{\boldsymbol{q}} - \tilde{L}(\boldsymbol{q},\boldsymbol{p}) = p_1\dot{q}_1 + p_2\dot{q}_2 + p_3\dot{q}_3 + p_4\dot{q}_4 - \tilde{L}(\boldsymbol{q},\boldsymbol{p}) = \\ &p_1\dot{q}_1 + p_2\dot{q}_2 + p_3\dot{q}_3 + p_4\dot{q}_4 - \frac{\gamma}{2}\Big\{(\partial_X q_1 + \dot{q}_2 + q_3)^2 - \\ &2(1-\mu)\left[\partial_X q_1(\dot{q}_2 + q_3) - \frac{1}{4}(\dot{q}_1 + \partial_X q_2)^2\right]\Big\} - \\ &\frac{1}{2}\left\{(\partial_X^2 q_3 - \dot{q}_4)^2 + 2(1-\mu)\left[\dot{q}_4\partial_X^2 q_3 + \left(\partial_X q_4 - \frac{1}{2}\partial_X q_2\right)^2\right]\right\} - \\ &T_{cr}\dot{q}_3\partial_X q_3 + \frac{1}{4}(1+\gamma)(1-\mu)(\partial_X q_2)^2 - \frac{N_{cr}}{2}(\partial_X W)^2. \end{aligned} \tag{8}$$

将方程(7)代入变分方程

$$\delta\int[\boldsymbol{p}^{\mathrm{T}}\dot{\boldsymbol{q}} - H(\boldsymbol{q}, \boldsymbol{p})]\mathrm{d}\Omega = 0. \tag{9}$$

通过分部积分可以得到 Hamilton 正则方程

$$\dot{\boldsymbol{q}} = \frac{\delta H}{\delta \boldsymbol{p}},\ \dot{\boldsymbol{p}} = -\frac{\delta H}{\delta \boldsymbol{q}}, \tag{10}$$

即

$$\begin{Bmatrix} \dot{\boldsymbol{q}} \\ \dot{\boldsymbol{p}} \end{Bmatrix} = \begin{bmatrix} \boldsymbol{A} & \boldsymbol{B} \\ \boldsymbol{C} & -\boldsymbol{A}^{\mathrm{T}} \end{bmatrix} \begin{Bmatrix} \boldsymbol{q} \\ \boldsymbol{p} \end{Bmatrix}, \tag{11}$$

其中

$$\boldsymbol{A} = \begin{bmatrix} 0 & -\partial_X & 0 & 0 \\ -\mu\partial_X & 0 & -1 & 0 \\ 0 & 1 & 0 & -1 \\ 0 & 0 & \partial_X^2 & 0 \end{bmatrix},\ \boldsymbol{B} = \begin{bmatrix} 2/(\gamma(1-\mu)) & 0 & 0 & 0 \\ 0 & 1/\gamma & 0 & 0 \\ 0 & 0 & 0 & 0 \\ 0 & 0 & 0 & 1 \end{bmatrix},$$

$$\boldsymbol{C}=\begin{bmatrix} -\gamma(1-\mu^2)\partial_X^2 & 0 & 0 & 0 \\ 0 & -\frac{1-\mu}{2}\partial_X^2 & 0 & 0 \\ 0 & 0 & N_{\mathrm{cr}}\partial_X^2 & T_{\mathrm{cr}}\partial_X \\ 0 & 0 & -T_{\mathrm{cr}}\partial_X & 0 \end{bmatrix}.$$

令全状态向量 $\boldsymbol{\psi}=\{\boldsymbol{q}^{\mathrm{T}},\boldsymbol{p}^{\mathrm{T}}\}^{\mathrm{T}}$, 方程(11)简写为

$$\dot{\boldsymbol{\psi}}=\boldsymbol{H}\boldsymbol{\psi}, \tag{12}$$

其中 $\boldsymbol{H}$ 为 Hamilton 算子矩阵.

3 问题的辛本征值与辛本征解

在辛空间,方程的解可以表示为[9-10]

$$\boldsymbol{\psi}(X,\theta)=\sum\boldsymbol{\psi}_n(X)\mathrm{e}^{\lambda_n\theta}, \tag{13}$$

其中 λ_n 为算子矩阵 $\boldsymbol{H}$ 的本征值, $\boldsymbol{\psi}_n=\{\bar{q}_1,\bar{q}_2,\bar{q}_3,\bar{q}_4,\bar{p}_1,\bar{p}_2,\bar{p}_3,\bar{p}_4\}^{\mathrm{T}}$ 为其所对应的本征向量, 满足

$$\boldsymbol{H}\boldsymbol{\psi}_n=\lambda_n\boldsymbol{\psi}_n. \tag{14}$$

根据圆柱壳体端部条件 ($\theta=0$ 和 $\theta=2\pi$) 的连续性,边界条件满足

$$\bar{q}_i\big|_{\theta=0}=\bar{q}_i\big|_{\theta=2\pi},\ \bar{p}_i\big|_{\theta=0}=\bar{p}_i\big|_{\theta=2\pi}\qquad(i=1,2,3,4), \tag{15}$$

即 $\boldsymbol{\psi}_n(0)=\boldsymbol{\psi}_n(2\pi)$,因此算子矩阵 $\boldsymbol{H}$ 的本征值应满足 $\lambda_n=in$ ($n=0,\ \pm1,\ \pm2,\cdots$), 方程(13)可以写成

$$\boldsymbol{\psi}(X,\theta)=\sum\boldsymbol{\psi}_n(X)\mathrm{e}^{in\theta}. \tag{16}$$

将式(16)代入方程(14),特征方程转化为

$$in\boldsymbol{\psi}_n=\boldsymbol{H}\boldsymbol{\psi}_n. \tag{17}$$

令本征解为

$$\boldsymbol{\psi}_n=\boldsymbol{c}_1\mathrm{e}^{\xi_1X}+\boldsymbol{c}_2\mathrm{e}^{\xi_2X}+\boldsymbol{c}_3\mathrm{e}^{\xi_3X}+\boldsymbol{c}_4\mathrm{e}^{\xi_4X}+\boldsymbol{c}_5\mathrm{e}^{\xi_5X}+\boldsymbol{c}_6\mathrm{e}^{\xi_6X}+\boldsymbol{c}_7\mathrm{e}^{\xi_7X}+\boldsymbol{c}_8\mathrm{e}^{\xi_8X}, \tag{18}$$

其中 $\boldsymbol{c}_k=\{c_{1k},c_{2k},c_{3k},c_{4k},c_{5k},c_{6k},c_{7k},c_{8k}\}^{\mathrm{T}}(k=1,2,\cdots,8)$ 是常向量, $\xi_i(i=1,2,\cdots,8)$ 是特征方程的根,满足

$$\xi^8+a_1\xi^6+a_2\xi^5+a_3\xi^4+a_4\xi^3+a_5\xi^2+a_6\xi+a_7=0, \tag{19}$$

其中

$$\begin{cases} a_1=N_{\mathrm{cr}}-n^2[4\gamma+(5-\mu)/2]/(1+\gamma), \\ a_2=-2inT_{\mathrm{cr}}, \\ a_3=\gamma(1-\mu^2)+[n^4(2-\mu+6\gamma)-2n^2\gamma(2+\mu)-2n^2\gamma N_{\mathrm{cr}}]/(1+\gamma)- \\ \qquad N_{\mathrm{cr}}(5-2\mu+\mu^2)/((1+\gamma)(1-\mu)), \\ a_4=-inT_{\mathrm{cr}}[n^2(1+\mu-4\gamma)+2\gamma(2+\mu)]/(1+\gamma), \\ a_5=2n^4N_{\mathrm{cr}}-n^2[n^4(8\gamma+1-\mu)-2T_{\mathrm{cr}}^2- \\ \qquad 4n^2\gamma(3+\mu)+\gamma(5+3\mu)]/[2(1+\gamma)], \\ a_6=-2i\gamma T_{\mathrm{cr}}(n^5-n^3)/(1+\gamma), \\ a_7=\gamma(n^8-2n^6+n^4)/(1+\gamma). \end{cases} \tag{20}$$

$c_{mk}(m=1,2,\cdots,8)$ 满足

$$\begin{cases} c_{2k}=b_{1k}c_{1k}, \\ c_{3k}=b_{2k}c_{1k}, \\ c_{4k}=-inc_{3k}+c_{2k}, \\ c_{5k}=(1-\mu)\gamma(inc_{1k}+\xi_k c_{2k})/2, \\ c_{6k}=\gamma(inc_{2k}+c_{3k}+\mu\xi_k c_{1k}), \\ c_{7k}=[in(n^2-\xi_k^2)+\xi_k T_{\mathrm{cr}}]c_{3k}-n^2c_{2k}, \\ c_{8k}=(n^2-\xi_k^2)c_{3k}+inc_{2k}, \end{cases} \tag{21}$$

其中

$$b_{1k}=b_{4k}/b_{0k},$$
$$b_{2k}=b_{5k}+b_{1k}b_{3k},$$
$$b_{0k}=T_{\mathrm{cr}}\xi_k^2n^2(1+\mu)+in\xi_k[\gamma(1-\mu)-2\mu(n^2-\xi_k^2)+(1+\mu)(n^2-\xi_k^2)^2]/2,$$
$$b_{3k}=(1+\mu)in\xi_k/(2\mu\xi_k),$$
$$b_{4k}=inT_{\mathrm{cr}}\xi_k(2\xi_k^2-n^2+\mu n^2)+\gamma n^2(1-\mu)/2+$$
$$(n^2-\mu n^2-2\xi_k^2)(n^2-\xi_k^2)^2/2+\xi_k^2\gamma(\mu^2-1),$$
$$b_{5k}=[\xi_k^2-(1-\mu)n^2/2]/(\mu\xi_k).$$

在式(21)中，b_{1k}，b_{2k} 是 c_{mk} 的系数，这个系数的值又跟其他的 b_{0k}，b_{3k}，b_{4k}，b_{5k} 有关系，与 m 的取值无关，在这不做特别说明。

当 $n=0$ 时，特征方程的系数只有 a_1 和 a_3 不为0，且这两项系数只跟 N_{cr} 有关系，即应力波传播时与扭转载荷没有影响，这同圆柱壳受耦合冲击相矛盾，因此与圆柱壳扭转屈曲一样，受耦合冲击的圆柱壳也不会发生轴对称屈曲。

4 Hamilton 体系下的边界条件和分叉条件

在轴向和扭转耦合应力波冲击下，圆柱壳可分为应力传播区：包含轴向压缩和扭转应力波共同作用区（区域1）、轴向压缩应力波作用区（区域2）和载荷未扰动区（区域3）。

本征解在冲击端（$X=0$）应满足的端部条件用 Hamilton 体系下的混合变量描述如下：

$$\begin{cases} q_1[(1-\mu^2)\partial_X q_1+\mu p_2/\gamma]=0, \\ q_2[-\partial_X q_2+2\partial_X q_4+2p_1/(1-\mu)+2T_{\mathrm{cr}}q_3/(1-\mu)]=0, \\ q_3[-2\mu\partial_X^2 q_1-2\partial_X q_3-\partial_X p_4+2\partial_X p_2/\gamma+N_{\mathrm{cr}}\partial_X q_3-T_{\mathrm{cr}}(q_2-q_4)]=0, \\ \partial_X q_3[(1-\mu)\partial_X^2 q_3-\mu p_4]=0. \end{cases} \tag{22}$$

式(22)包括了各种端部边界条件，考虑固支端部边界条件：

$$q_1=0,\ q_2=0,\ q_3=0,\ \partial_X q_3=0.$$

本征解在轴向压缩和扭转应力波共同作用波阵面（$X_{\mathrm{r}}=c_2t$），即区域1和区域2的交界，应满足连续性条件：

$$
\begin{cases}
q_1^{(1)}|_{X=X_r^-} = q_1^{(2)}|_{X=X_r^+}, \\
q_2^{(1)}|_{X=X_r^-} = q_2^{(2)}|_{X=X_r^+}, \\
q_3^{(1)}|_{X=X_r^-} = q_3^{(2)}|_{X=X_r^+}, \\
\partial_X q_3^{(1)}|_{X=X_r^-} = \partial_X q_3^{(2)}|_{X=X_r^+}, \\
(1-\mu^2)\partial_X q_1^{(1)}|_{X=X_r^-} + \mu p_2^{(1)}|_{X=X_r^-}/\gamma = \\
\qquad (1-\mu^2)\partial_X q_1^{(2)}|_{X=X_r^+} + \mu p_2^{(2)}|_{X=X_r^+}/\gamma, \\
-\partial_X q_2^{(1)}|_{X=X_r^-} + 2\partial_X q_4^{(1)}|_{X=X_r^-} + 2p_1^{(1)}|_{X=X_r^-}/(1-\mu) + \\
\qquad 2T_{cr} q_3^{(1)}|_{X=X_r^-}/(1-\mu) = \\
\qquad -\partial_X q_2^{(2)}|_{X=X_r^+} + 2\partial_X q_4^{(2)}|_{X=X_r^+} + 2p_1^{(2)}|_{X=X_r^+}/(1-\mu), \\
-2\mu\partial_X^2 q_1^{(1)}|_{X=X_r^-} - 2\partial_X q_3^{(1)}|_{X=X_r^-} - \partial_X p_4^{(1)}|_{X=X_r^-} + 2\partial_X p_2^{(1)}|_{X=X_r^-}/\gamma + \\
\qquad N_{cr}\partial_X q_3^{(1)}|_{X=X_r^-} - T_{cr}(q_2^{(1)}|_{X=X_r^-} - q_4^{(1)}|_{X=X_r^-}) = \\
\qquad -2\mu\partial_X^2 q_1^{(2)}|_{X=X_r^+} - 2\partial_X q_3^{(2)}|_{X=X_r^+} - \partial_X p_4^{(2)}|_{X=X_r^+} + \\
\qquad 2\partial_X p_2^{(2)}|_{X=X_r^+}/\gamma + N_{cr}\partial_X q_3^{(2)}|_{X=X_r^+}, \\
-\mu p_4^{(1)}|_{X=X_r^-} + (1-\mu)\partial_X^2 q_3^{(1)}|_{X=X_r^-} = \\
\qquad -\mu p_4^{(2)}|_{X=X_r^+} + (1-\mu)\partial_X^2 q_3^{(2)}|_{X=X_r^+}.
\end{cases}
\tag{23}
$$

在载荷未扰动区,内力和位移均为0,所以在波前($X = X_e < L$)应满足连续性条件:

$$q_1 = 0,\ q_2 = 0,\ q_3 = 0,\ \partial_X q_3 = 0 \qquad (X = X_e). \tag{24}$$

本征解应满足边界条件和连续性条件,由本征解(18),边界条件(24)可以写成

$$[\boldsymbol{A}]_{16\times16}\boldsymbol{c} = \boldsymbol{0}, \tag{25}$$

其中

$$
\begin{aligned}
&A_{1k} = 1,\ A_{2k} = b_{1k},\ A_{3k} = b_{2k},\ A_{4k} = \xi_k b_{2k}, \\
&A_{5k} = [\xi_k + \mu(inb_{1k} + b_{2k})]e^{\xi_k X_r}, \\
&A_{6k} = [\gamma in + (1+\gamma)\xi_k b_{1k} - 2in\xi_k b_{2k}]e^{\xi_k X_r}, \\
&A_{7k} = [\xi_k^3 b_{2k} - \mu(n^2\xi_k b_{2k} + in\xi_k b_{1k}) + N_{cr}\xi_k b_{2k} - inT_{cr} b_{2k}]e^{\xi_k X_r}, \\
&A_{8k} = [\xi_k^2 b_{2k} - \mu(n^2 b_{2k} + inb_{1k})]e^{\xi_k X_r}, \\
&A_{9k} = -[\xi_k + \mu(inb_{1k} + b_{2k})]e^{\xi_k X_r}, \\
&A_{10k} = -[\gamma in + (1+\gamma)\xi_k b_{1k} - 2in\xi_k b_{2k}]e^{\xi_k X_r}, \\
&A_{11k} = -[\xi_k^3 b_{2k} - \mu(n^2\xi_k b_{2k} + in\xi_k b_{1k}) + N_{cr}\xi_k b_{2k}]e^{\xi_k X_r}, \\
&A_{12k} = -[\xi_k^2 b_{2k} - \mu(n^2 b_{2k} + inb_{1k})]e^{\xi_k X_r}, \\
&A_{13k} = e^{\xi_k X_e},\ A_{14k} = b_{1k}e^{\xi_k X_e},\ A_{15k} = b_{2k}e^{\xi_k X_e},\ A_{16k} = \xi_k b_{2k}e^{\xi_k X_e}.
\end{aligned}
$$

如果本征解恒为0,圆柱壳不发生前屈曲,因此,本征解有非零解.要求系数行列式 $|\boldsymbol{A}|$ 为0,即分叉条件为

$$|\boldsymbol{A}| = 0. \tag{26}$$

从分叉条件可求解出圆柱壳轴向冲击载荷 N_{cr} 与扭转冲击载荷 T_{cr} 之间的关系,在某一时刻相应的屈曲模态由方程(26)及本征解(18)得到.

5　数值结果

由分叉条件(26)经过数值计算得到了临界屈曲载荷曲线，由式(16)、(18)得到相应的屈曲模态．针对冲击端固支和简支的情况，对轴向和扭转耦合冲击载荷作用下的弹性圆柱壳进行数值计算，其中无量纲化后的圆柱壳尺寸：壁厚 $\bar{h} = h/R$．所计算圆柱壳的尺寸：$\bar{h} = 0.05$，Poisson 比 $\mu = 0.25$．

长圆柱壳在轴向和扭转耦合载荷冲击下，对于给定的扭转冲击载荷 T_{cr}，都能得到轴向临界载荷随波阵面的变化曲线以及相应的屈曲模态．临界曲线及屈曲模态同样分为两类：局部屈曲和整体屈曲．

对冲击端固支的情况：

1) $n \neq 1$ 时临界屈曲载荷曲线与屈曲模态

图 2 给出了 $n = 3$，$T_{cr} = 20$ 时轴向临界载荷随波阵面的变化曲线($n = 3$，$T_{cr} = 30$ 时轴向临界载荷随波阵面的变化曲线参见图 5)．从图中可以看出，随着波阵面的传播，有的临界载荷曲线逐渐下降并趋于一固定值，有的相邻不同分支的临界载荷曲线呈现绞扭趋势下降并逐渐趋于不同的固定值．对于相同阶数，波传播到相同波阵面，临界载荷值同只承受轴向冲击作用相比要小，这说明耦合冲击作用下的圆柱壳更易于发生屈曲．对于同一阶受耦合冲击的圆柱壳，施加扭转载荷较大时所需要的轴向临界载荷则小．

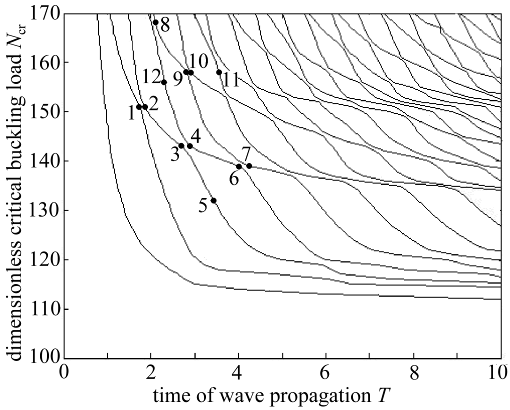

图 2　当 $n = 3$，$T_{cr} = 20$ 时轴向临界载荷随波阵面的曲线

Fig.2　The axial critical buckling loads with time of wave front propagation ($n = 3$, $T_{cr} = 20$)

图 3 给出了 $n = 3$，$T_{cr} = 20$，当 $N_{cr} = 145$ 时前 6 分支的屈曲模态；图 4 给出了 $n = 3$，$T_{cr} = 20$ 时不同波阵面的屈曲模态，分别对应图 2 中标出的波传播位置．由于应力横波比纵波波速慢，圆柱壳在轴扭耦合载荷冲击作用下被分成 3 个区域：轴扭耦合作用区、轴向冲击作用区和未扰动

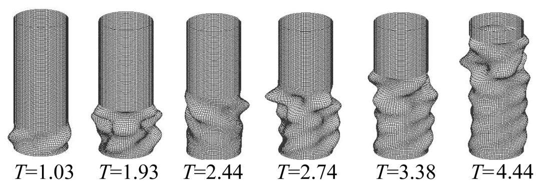

图 3　当 $N_{cr} = 145$ 时前 6 分支的屈曲模态 ($n = 3$，$T_{cr} = 20$)

Fig.3　The critical buckling modes of the first 6 branches when $N_{cr} = 145$ ($n = 3$, $T_{cr} = 20$)

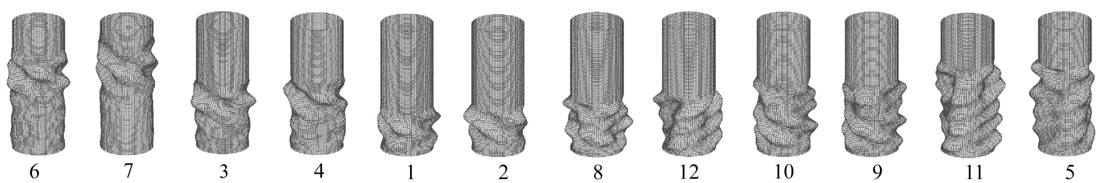

图 4　当 $n = 3$，$T_{cr} = 20$ 时不同波阵面的屈曲模态

Fig.4　Some buckling modes with different wave front propagation ($n = 3$, $T_{cr} = 20$)

区.阶数 n 对应环向波纹数,分支数 m 对应轴向波纹数,随着应力纵波和横波的发展,圆柱壳的轴向波纹数增加.

图 5 给出了 $n = 3, T_{cr} = 30$ 时轴向临界载荷随波阵面的变化曲线;图 6 给出了当 $n = 3, T_{cr} = 30$ 时,第 1 分支不同波阵面的屈曲模态;图 7 给出了 $n = 3, T_{cr} = 30$,当 $N_{cr} = 140$ 时前 6 分支的屈曲模态.

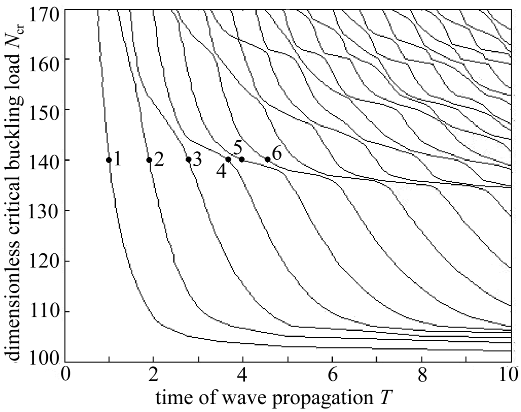

图 5 当 $n = 3, T_{cr} = 30$ 时轴向临界载荷随波阵面的曲线

Fig.5 The axial critical buckling loads with time of wave front propagation ($n = 3, T_{cr} = 30$)

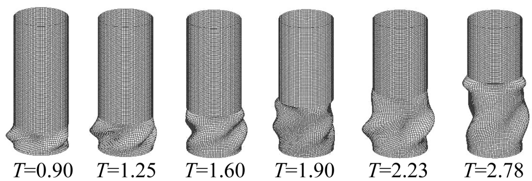

图 6 第 1 分支不同波阵面的屈曲模态($n = 3, T_{cr} = 30$)

Fig.6 The critical buckling modes of the first branch with different wave front propagation ($n = 3, T_{cr} = 30$)

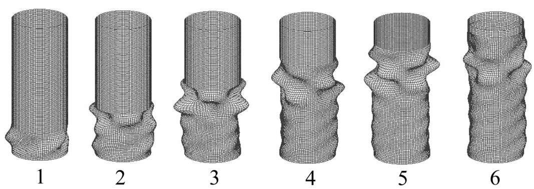

图 7 当 $N_{cr} = 140$ 时前 6 分支的屈曲模态($n = 3, T_{cr} = 30$)

Fig.7 The critical buckling modes of the first 6 branches when $N_{cr} = 140$ ($n = 3, T_{cr} = 30$)

2) $n = 1$ **临界屈曲载荷曲线与屈曲模态**

图 8 给出了当 $n = 1, T_{cr} = 20$ 时轴向临界载荷随波阵面的曲线,从图中可以看出临界载荷曲线分为两类:一类是曲线随着波阵面的传播临界载荷值迅速下降趋于平缓逐渐接近于一固定值,另一类是波阵面传播到一定阶段,临界载荷迅速下降并接近于 0.在此称第 1 类为局部屈曲载荷曲线,第 2 类为整体屈曲载荷曲线.

图 9 给出了 $n = 1, T_{cr} = 20$,当 $N_{cr} = 166$ 时前 6 分支的屈曲模态.图 10 给出了 $n = 1, T_{cr} = 20$ 时不同波阵面的整体屈曲模态,分别对应第 2 类曲线上相应的传播位置.从图中可以看出,在第 1 类局部屈曲载荷曲线上对应的屈曲模态与非一阶的屈曲模态相类似,区别只是环向波纹数不同.第 2 类整体屈曲载荷曲线上对应的屈曲模态,在轴扭耦合区域主要体现耦合的整体

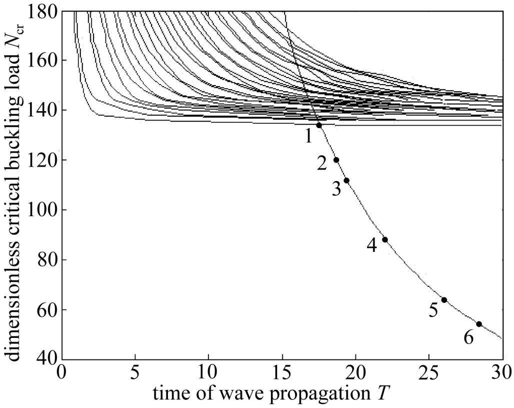

图 8　当 $n = 1$, $T_{cr} = 20$ 时轴向临界载荷随波阵面的曲线

Fig.8　The axial critical buckling loads with time of wave front propagation ($n = 1$, $T_{cr} = 20$)

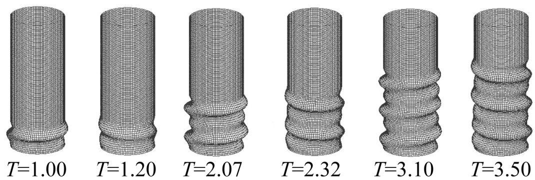

图 9　当 $N_{cr} = 166$ 时前 6 分支的屈曲模态 ($n = 1$, $T_{cr} = 20$)

Fig.9　The critical buckling modes of the first 6 branches when $N_{cr} = 166$ ($n = 1$, $T_{cr} = 20$)

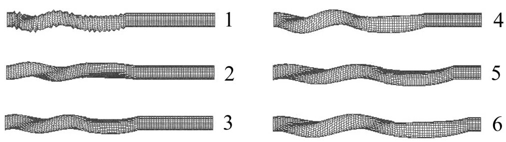

图 10　当 $n = 1$, $T_{cr} = 20$ 时不同波阵面的整体屈曲模态

Fig.10　Some global buckling modes with different wave front propagation ($n = 1$, $T_{cr} = 20$)

屈曲模态,在轴向冲击作用区体现整体弯曲屈曲.在图 10 中点 1 处的屈曲模态又与其它点处不同.点 1 位于两类曲线的交点处,此点处的屈曲模态为局部屈曲和整体屈曲的耦合屈曲模态.

对冲击端简支的情况:

1) $n \neq 1$ 临界屈曲载荷曲线与屈曲模态

图 11 给出了当 $n = 3$, $T_{cr} = 20$ 时轴向临界载荷随波阵面的变化曲线;图 12 给出了 $n = 3$, $T_{cr} = 20$, 当 $N_{cr} = 138$ 时前 6 分支的屈曲模态.从图中可以看出,冲击端简支时仍存在固定的扭转冲击载荷下,轴向冲击临界载荷随着波阵面的传播逐渐下降并趋于不同的固定值.对于相同波阵面,施加扭转载荷较大时所需要的轴

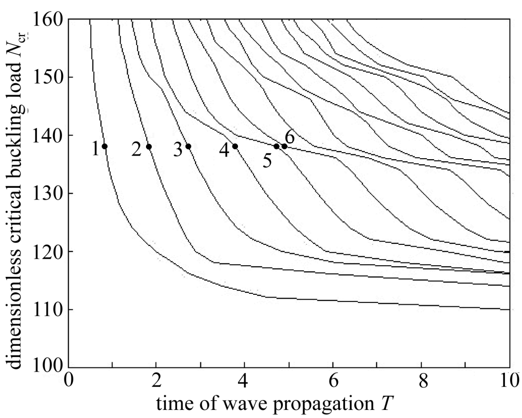

图 11　当 $n = 3$, $T_{cr} = 20$ 时轴向临界载荷随波阵面的曲线

Fig.11　The axial critical buckling loads with time of wave front propagation ($n = 3$, $T_{cr} = 20$)

向临界载荷则小.

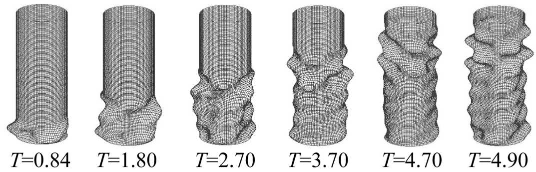

图 12 当 $N_{cr}=138$ 时前 6 分支的屈曲模态（$n=3$, $T_{cr}=20$）

Fig.12 The critical buckling modes of the first 6 branches when $N_{cr}=138$ ($n=3$, $T_{cr}=20$)

2）$n=1$ 临界屈曲载荷曲线与屈曲模态

图 13 给出了 $n=1$, $T_{cr}=20$ 时轴向临界载荷随波阵面的曲线.与冲击端固支一样,临界载荷曲线也分为两类:一类是曲线随着波阵面的传播临界载荷值迅速下降趋于平缓逐渐接近于一固定值,另一类是波阵面传播到一定阶段,临界载荷迅速下降并接近于 0.同样称第 1 类为局部屈曲载荷曲线,第 2 类为整体屈曲载荷曲线.与冲击端固支不同的是临界载荷曲线并没有绞扭着逐渐下降.

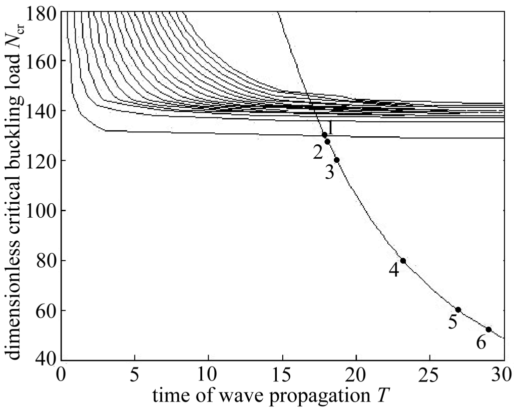

图 13 当 $n=1$, $T_{cr}=20$ 时轴向临界载荷随波阵面的曲线

Fig.13 The axial critical buckling loads with time of wave front propagation ($n=1$, $T_{cr}=20$)

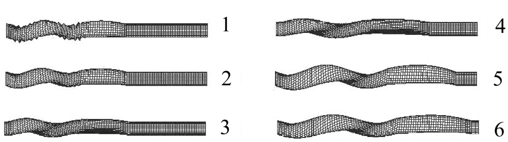

图 14 当 $n=1$, $T_{cr}=20$ 时不同波阵面的整体屈曲模态

Fig.14 Some global buckling modes with different wave front propagation ($n=1$, $T_{cr}=20$)

图 14 给出了当 $n=1$, $T_{cr}=20$ 时不同波阵面的整体屈曲模态,分别对应第 2 类曲线上相应传播位置.与冲击端固支情况类似,屈曲模态也分为两类.第 1 类是局部屈曲载荷曲线上对应的屈曲模态,与非一阶的屈曲模态相类似,区别只是环向波纹数不同.第 2 类是整体屈曲载荷曲线上对应的屈曲模态,在轴扭耦合区域主要体现耦合的整体屈曲模态,在轴向冲击作用区体现整体弯曲屈曲.在图 14 中,点 1 处的屈曲模态又与其它点处不同.点 1 位于两类曲线的交点处,此点处的屈曲模态为局部屈曲和整体屈曲的耦合屈曲模态.

6 结 论

在 Hamilton 体系下,轴扭耦合载荷冲击下长圆柱壳的临界屈曲载荷和屈曲模态归结为辛本征值和本征解问题.在轴扭耦合载荷冲击下辛本征值只能取非零值,因此长圆柱壳只能发生非轴对称动态屈曲问题.阶数 n 对应环向波纹数,分支数 m 对应轴向波纹数,随着应力纵波和横波的发展,圆柱壳的轴向波纹数增加.由于纵波和横波的传播速度不同,长圆柱壳的屈曲分为 3 个区域:耦合作用区、轴向冲击作用区和未扰动区.长圆柱壳阶数 $n \neq 1$ 时发生局部屈曲,阶数 $n = 1$ 时会发生局部屈曲、整体屈曲以及局部与整体的耦合屈曲.

参考文献(References):

[1] Bisagni C, Cordisco C. An experimental investigation into the buckling and post-buckling of CFRP shells under combined axial and torsion loading[J]. *Composite Structures*, 2003, **60**(4): 391-402.

[2] Bisagni C, Cordisco P. Post-buckling and collapse experiments of stiffened composite cylindrical shells subjected to axial loading and torque[J]. *Composite Structures*, 2006, **73**(2): 138-149.

[3] Miyazaki N. Creep buckling analysis of circular cylindrical shell under both axial compression and internal or external pressure[J]. *Composite Structures*, 1988, **28**(4): 437-441.

[4] Azam T. Delaminating buckling and post buckling in composite cylindrical shells under combined axial compression and external pressure[J]. *Composite Structures*, 2006,**72**(4): 401-418.

[5] Diaconu C G, Sato M, Sekine H. Buckling characteristics and layup optimization of long laminated composite cylindrical shells subjected to combined loads using lamination parameters [J]. *Composite Structures*, 2002, **58**(4): 423-433.

[6] 黄承义, 刘土光, 郑际嘉. 圆柱壳在径向冲击载荷作用下的弹性脉冲屈曲[J].应用数学和力学, 1996, **17**(8): 735-741.(HUANG Cheng-yi, LIU Tu-guang, ZHENG Ji-jia. Elastic pulse buckling of cylindrical shells under radial impulsive loading[J]. *Applied Mathematics and Mechanics*, 1996, **17**(8): 735-741.(in Chinese))

[7] 吴斌, 韩强, 杨桂通. 正交异性圆柱壳受冲扭联合作用的弹性波传播[J]. 北京工业大学学报, 1999, **25**(4): 23-28, 34.(WU Bing, HAN Qiang, YANG Gui-tong. Action of axial impact and torsion[J]. *Journal of Beijing Polytechnic University*, 1999, **25**(4): 23-28, 34.(in Chinese))

[8] 王德禹, 张善元, 杨桂通. 刚塑性圆柱壳的冲击扭转屈曲[J]. 应用数学和力学, 1993, **14**(8): 659-664.(WANG De-yu, ZHANG Shan-yuan, YANG Gui-tong. The impact torsional buckling for the rigid plastic cylindrical shell[J]. *Applied Mathematics and Mechanics*, 1993, **14**(8): 659-664.(in Chinese))

[9] 姚伟岸, 钟万勰. 辛弹性力学[M]. 北京: 高等教育出版社, 2002.(YAO Wei-an, ZHONG Wan-xie. *Symplectic Elasticity*[M]. Beijing: Higher Education Press, 2002.(in Chinese))

[10] XU Xin-sheng, MA Yuan, Lim C W, CHU Hong-jie. Dynamic buckling of cylindrical shells subject to an axial impact in a symplectic system[J]. *International Journal of Solids and Structures*, 2006, **43**(13): 3905-3919.

Dynamic Buckling of Cylindrical Shells Under Coupled Impact Loads

MA Jian-qing[1], XU Xin-sheng[2]

(1. *Mechanical Engineering College*, *Xi' an Shiyou University*, *Xi' an* 710065, *P.R.China*;

2. *State Key Laboratory of Structural Analysis for Industrial Equipment*; *Department of Engineering Mechanics*, *Dalian University of Technology*, *Dalian*, *Liaoning* 116024, *P.R.China*)

Abstract: In consideration of the stress wave propagation under axial-torsional coupled impact loads, the dynamic buckling of elastic long cylindrical shells was investigated. The Hamiltonian system for the problem was established firstly. Then, accordingly, the critical buckling loads and buckling modes were converted to a problem of eigenvalues and eigensolutions in the symplectic space. By means of the Hamiltonian system a perfect buckling space was given, and the relations of how the critical loads and buckling modes corresponded to the symplectic eigenvalues and eigensolutions in the symplectic space were revealed. Due to the different propagation velocities of the axial stress wave and torsional stress wave, progress and reflection of the longitudinal wave and transverse wave were not synchronous within a cylindrical shell. So the cylindrical shell was divided into three regions with respective different stress, displacement and boundary conditions. The numerical results of critical load curves and buckling modes under clamped and simple boundary conditions were given. Especially, the different first-order buckling modes were discussed detailedly.

Key words: Hamiltonian system; cylindrical shell; dynamic buckling; coupled impact; stress wave